

Extreme ultraviolet microexposures at the Advanced Light Source using the 0.3 numerical aperture micro-exposure tool optic

Patrick P. Naulleau,^{a)} Kenneth A. Goldberg, and Erik Anderson
Center for X-Ray Optics, Lawrence Berkeley National Laboratory, Berkeley, California 94720

Jason P. Cain
EECS Department, University of California, Berkeley, California 94720

Paul Denham, Keith Jackson, Anne-Sophie Morlens, Seno Rekawa, and Farhad Salmassi
Center for X-Ray Optics, Lawrence Berkeley National Laboratory, Berkeley, California 94720

(Received 16 June 2004; accepted 2 August 2004; published 10 December 2004)

In an effort to continue the rapid pace of extreme ultraviolet (EUV) learning, the focus of developmental EUV lithography has shifted from low numerical aperture (NA) tools such as the 0.1 NA engineering test stand to higher NA tools such as the 0.3 NA micro-exposure tool (MET). To support this generation of lithographic optics, a static printing station has been developed at the Advanced Light Source. This synchrotron-based printing system relies on a scanning illuminator to provide real-time coherence (pupil-fill) control. Here, we describe a MET printing station and present early printing results obtained with the Sematech Set-2 MET optic. The resolution limit of baseline EUV resist is presented as well as 30 nm equal-line-space printing in an experimental resist. © 2004 American Vacuum Society. [DOI: 10.1116/1.1802851]

I. INTRODUCTION

Extreme ultraviolet (EUV) lithography¹ is a leading candidate for volume production at the 32 nm node. To make this a reality, advanced research tools operating with numerical apertures (NAs) of 0.25 or greater are required today. Microfield exposure tools²⁻⁴ have been crucial to EUV development in the past and currently serve as the only source for high-NA EUV printing. Although not well-suited for manufacturing applications, synchrotron radiation provides an efficient, well-characterized, debris-free source for such microfield systems.^{3,4} As previously described,⁴ a significant issue with synchrotron sources, however, is the intrinsically high coherence of the source^{5,6} as compared to the reduced coherence requirements of a lithographic tool. The coherence issue has been overcome in the past through the use of active illuminator components.⁷

In this article, we describe the 0.3 NA EUV lithography capabilities at Lawrence Berkeley National Laboratory's Advanced Light Source (ALS) synchrotron radiation facility. This static microfield exposure station utilizes International Sematech's 0.3 NA micro-exposure tool (MET) optic.^{8,9} The MET optic is a centrally obscured two-element, axially symmetric 5 \times -reduction optical system manufactured by Zeiss. The central obscuration has a radius of 30% producing an annular pupil. To support reflective masks with this on-axis system, the mask is tilted by 4° and the wafer by 0.8°. The MET has a well-corrected field of view of 1 \times 3 mm at the reticle plane (200 \times 600 μ m at the wafer plane).

II. SYSTEM CONFIGURATION

The MET lithography station at Berkeley is based in large part on the previously implemented 0.1 NA static exposure

station;¹⁰ however, the 3 \times -larger NA has dictated the design and implementation of several subsystems, including stages, focus control, and sensing, as well as illumination. The computer-aided design model shown in Fig. 1 depicts the major exposure station components as well as the EUV beam path (the system is described in detail in Ref. 11). Effectively coherent radiation from undulator beamline 12^{5,6} at the ALS impinges on the scanning illuminator. The light is directed to a reflective reticle installed onto a five-axis stage mounted at an angle of 4°. From there the light is re-imaged by the MET optic with 5 \times demagnification to the wafer plane. A grazing incidence laser system is used to monitor the height of the wafer at the print site ensuring that it remains in focus. With the wafer removed, the light propagates to a scintillator plate sitting effectively in the far field. Pupil-fill monitoring is achieved by re-imaging the scintillator plate through a vacuum window to a visible-light CCD camera.

Although based on the same principle as the scanning illuminator used in the 0.1 NA static micro-exposure station,^{3,7,10} the illuminator used here was completely redesigned to support the larger NA and field size as well as a targeted decrease in exposure time.¹² The previous illuminator design supported a field of view of only 100 μ m, and exposure times of 4 s or longer were required due to limited scanning speeds. Figure 2 shows a schematic of the MET programmable coherence illuminator. The pupil-scanning capabilities are provided by two one-dimensional vacuum-compatible flexure suspension galvanometers.¹³ Using these high-speed one-dimensional scanners allows exposure times as short as 30 ms to be achieved for certain pupil fills. The pupil-scanner mirrors are both cylindrical, with power in the scanning direction. The curvatures are chosen to focus the incoming undulator radiation to the front focal plane of the toroidal condenser mirror used to re-image the two scanners

^{a)}Electronic mail: pnaulleau@lbl.gov

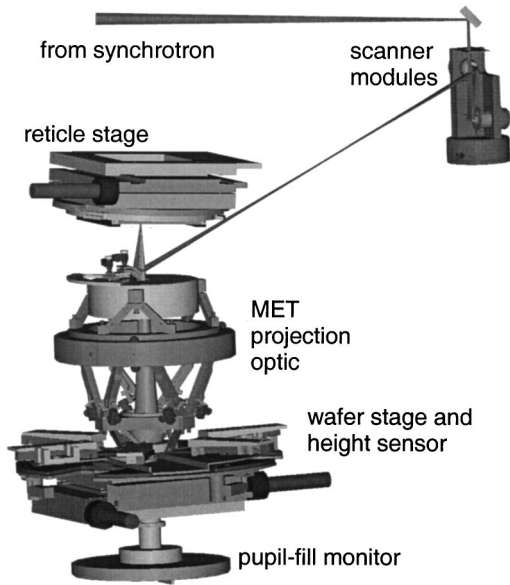


FIG. 1. Model depicting the major exposure station components and the EUV beam path (the system is described in detail in Ref. 11).

to the reticle. This characteristic provides for illumination stationarity across the $200 \times 600 \mu\text{m}$ field of view.¹² In addition to the two one-dimensional pupil scanners, the MET illuminator also includes a two-dimensional field uniformity scanner comprised of a flat mirror. This scanning mirror is used to improve the short-range uniformity of the illumination, but is not intended to synthesize the illumination field size.

Figure 3 shows a series of EUV pupil fills recorded using the pupil-fill monitor. In the large annular $0.35 < \sigma < 0.85$ illumination case, we see the onset of vignetting in the y direction, as evidenced by the squaring off of the pupil fill. This effect is due to the limited extent of the toroid in the y direction. The size of the toroid was constrained to prevent obscuration of imaging rays leaving the reticle and entering

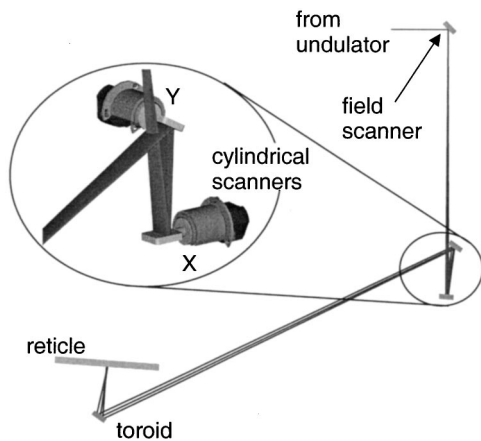


FIG. 2. Schematic of the MET programmable coherence illuminator. The pupil-scanner mirrors are both cylindrical with power in the scanning direction. In addition to the pupil scanners, the illuminator includes a 2D field uniformity scanner.

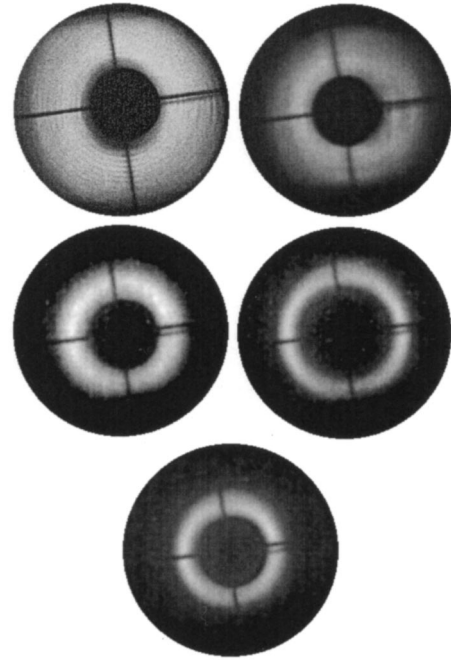


FIG. 3. Series of EUV pupil fills recorded using the pupil-fill monitor. The apparent vignetting of the pupil fills in the second row is an artifact of the pupil-fill monitor, which depending on the wafer stage position is partially obscured by a wire in the beam path.

the MET optic. This limitation does not exist in the x direction, where the toroid supports $\sigma=1$. The apparent vignetting of the pupil fills in the second row of Fig. 3 is an artifact of the pupil-fill monitor, which, depending on the wafer stage position, is partially obscured by a wire in the beam path. In the pupil-fill monitor images, we also see the MET central obscuration as well as the arms used to support the direct-transmission-blocking baffles. Although we show only annular pupil fills, the illuminator is not limited to synthesizing circular fills: the use of nonharmonic scanners allows arbitrary pupil fills to be generated within the limits of the physical extent of the toroid.

III. LITHOGRAPHIC PERFORMANCE CHARACTERIZATION

In order to serve as an effective research tool, the exposure system described above, combined with some baseline process, must be lithographically characterized. For the baseline resist process, we choose Rohm and Haas EUV two-dimensional (2D) resist. This resist material has been the mainstay of previous EUV work and is well characterized.¹⁴ A potentially significant concern with this resist, however, is its predicted resolution limit in the 40 to 45 nm range,^{15,16} whereas the MET optic has a Rayleigh resolution limit of 27 nm and can, in principle, print equal lines and spaces as small as 12 nm using dipole illumination. Figure 4 shows a series of equal-line-space patterns ranging from 90 down to 40 nm critical dimension (CD) printed in 125-nm-thick EUV-2D resist. Annular illumination with an inner σ of 0.3 and an outer σ of 0.7 was used. As predicted, the images

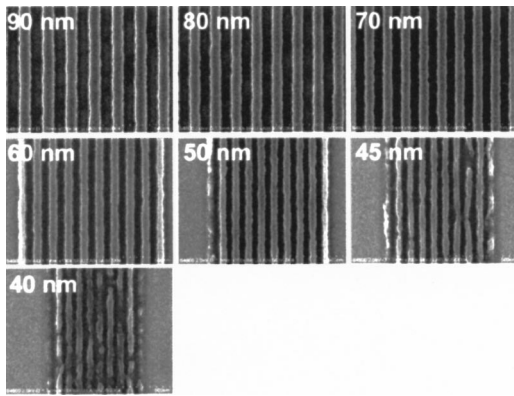


FIG. 4. Equal lines and spaces printed in 125-nm-thick layer of Rohm and Haas EUV-2D resist. The pupil fill was annular 0.3–0.7.

show the printing to breakdown in the 40 to 45 nm range. Figure 5 shows the measured CD and line-edge roughness (LER) through focus in 30 nm steps at best dose. The LER is reported as a single-sided 3σ value. These data reinforce the conclusions drawn from the single-image results in Fig. 4 and also demonstrates the fine focus control capabilities of the MET printing station.

Although the printing is observed to break down at approximately 40 nm, our conclusion of a resist limit assumes that the optic itself is capable of higher resolution. Theoretically this is true for an ideal 0.3 NA EUV optic, however, proving it requires a higher resolution resist. To this end, a set of experimental resists targeting high resolution at the expense of speed has been tested. Figure 6 shows a series of equal-line-space patterns printed in 125-nm-thick layer of MET 1-K resist provided by Rohm and Haas. The illumination conditions are the same as for the images in Fig. 4 (annular 0.3–0.7). Figure 7 again shows the CD and LER through focus at best dose. This experimental chemically amplified resist shows that the optic is capable of at least 30 nm printing and serves to verify the assertion that the printing limits observed in Figs. 4 and 5 are indeed due to the resist, and not the aerial image.

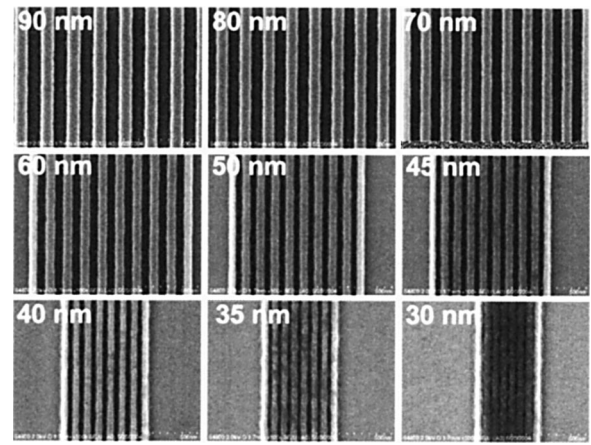


FIG. 6. Equal lines and spaces printed in 125-nm-thick layer of Rohm and Haas 1 K resist. The pupil fill was annular 0.3–0.7.

Because scanning electron microscopy collection of the full exposure-dose printing data has not yet been completed, it is difficult to rigorously quantify the depth of focus (DOF). However, assuming the LER to be proportional to the image log slope, we can use the through-focus LER to provide an estimate of the DOF. We believe that the flat LER behavior observed near focus on the larger CDs is a manifestation of the LER limits of the resists themselves. Using 10 nm LER as the cutoff for DOF yields the results presented in Fig. 8 for the two resists described above. In MET 1-K resist, the smallest CD at which we can measure a DOF is 35 nm, where we see a DOF of approximately 100 nm. In the EUV-2D resist, the smallest CD at which we can measure a DOF is only 50 nm, where we see a DOF of slightly less than 100 nm. MET 1-K resist provides a resolution improvement of approximately 15 nm.

IV. SUMMARY

The MET-based microfield exposure station is now operational at Lawrence Berkeley National Laboratory. This synchrotron-based system includes a programmable coher-

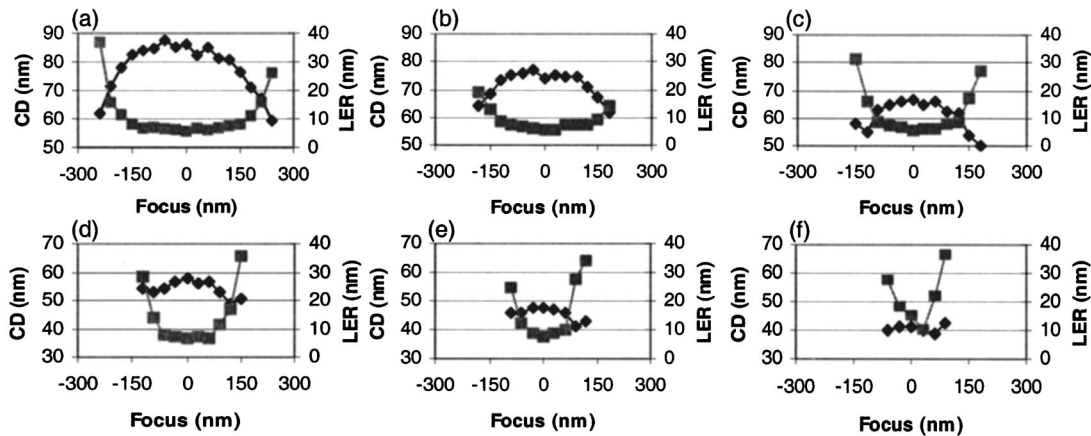


FIG. 5. Through focus (30 nm steps) CD and LER for lines and spaces printed in 125-nm-thick layer of EUV-2D resist. In all cases the features are equal lines and spaces with designed CDs of (a) 90, (b) 80, (c) 70, (d) 60, (e) 50, and (f) 45 nm. The diamond markers represent CD and the square markers LER.

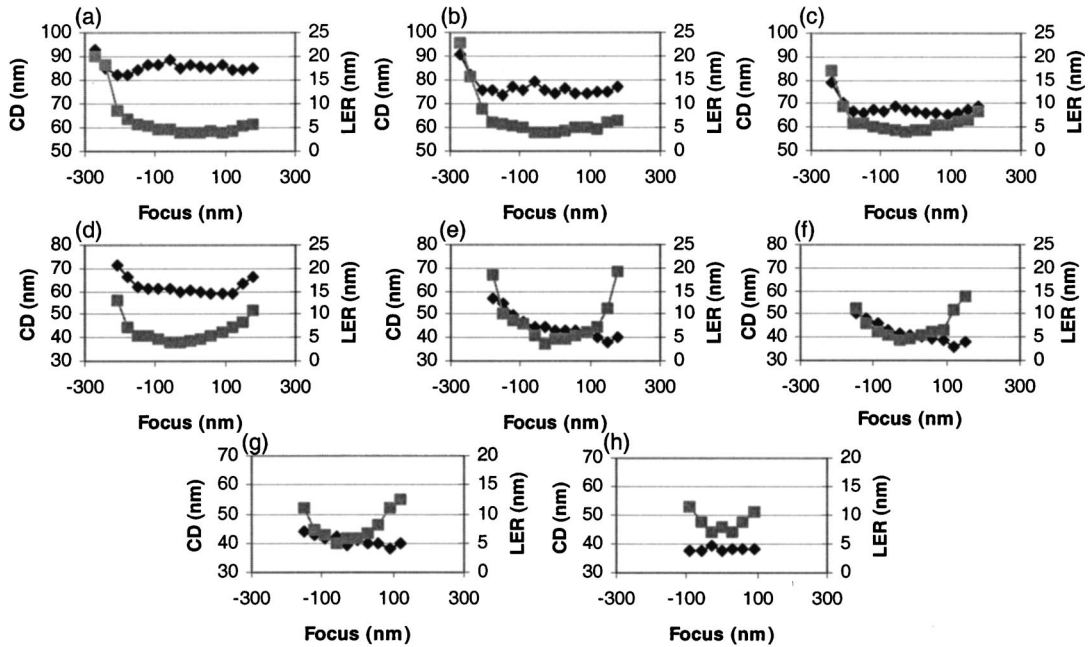


FIG. 7. Through-focus (30 nm steps) CD and LER for lines and spaces printed in 125-nm-thick layer of 1 K resist. In all cases, the features are equal lines and spaces with designed CDs of (a) 90, (b) 80, (c) 70, (d) 60, (e) 50, (f) 45, (g) 40, and (h) 35 nm. The diamond markers represent CD and the square markers LER.

ence illuminator, in principle, enabling the optic to achieve 12 nm equal-line-space printing. While still undergoing system-level optimization and characterization, the printing station has already provided early resist learning. The approximately 40 nm resolution limit of EUV-2D resist has been verified. Using an experimental chemically amplified resist, 30 nm equal-line-space printing has been demonstrated.

ACKNOWLEDGMENTS

The authors are greatly indebted to Kim Dean of International Sematech for project level and experimental support. Special thanks are due to Robert Brainard of Rohm and Haas for providing resist materials as well as expert processing support. We also acknowledge the entire CXRO staff for

enabling this research. This research was performed at Lawrence Berkeley National Laboratory and supported by International Sematech. Lawrence Berkeley National Laboratory is operated under the auspices of the Director, Office of Science, Office of Basic Energy Science, of the US Department of Energy.

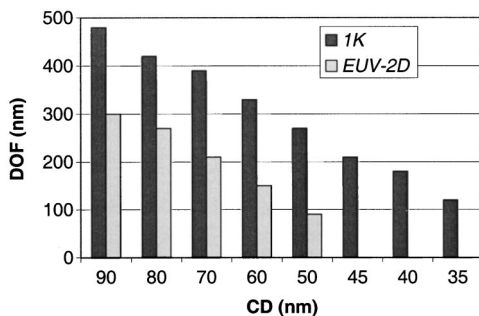


FIG. 8. DOF predicted from 10 nm threshold on through-focus LER data.

- ¹R. Stulen and D. Sweeney, *IEEE J. Quantum Electron.* **35**, 694 (1999).
- ²J. Goldsmith et al., *Proc. SPIE* **3676**, 264 (1999).
- ³K. Hamamoto, T. Watanabe, H. Tsubakino, H. Kinoshita, T. Shoki, and M. Hosoya, *J. Photopolym. Sci. Technol.* **14**, 567 (2001).
- ⁴P. Naulleau et al., *J. Vac. Sci. Technol. B* **20**, 2829 (2002).
- ⁵D. Attwood et al., *Appl. Opt.* **32**, 7022 (1993).
- ⁶C. Chang, P. Naulleau, E. Anderson, and D. Attwood, *Opt. Commun.* **182**, 24 (2000).
- ⁷P. Naulleau, K. Goldberg, P. Batson, J. Bokor, P. Denham, and S. Rekawa, *Appl. Opt.* **42**, 820 (2003).
- ⁸J. Taylor, D. Sweeney, R. Hudyma, L. Hale, T. Decker, G. Kubiak, W. Sweatt, and N. Wester, *Proceedings, 2nd International EUVL Workshop* (International Sematech, Austin, TX, 2000).
- ⁹R. Hudyma, J. Taylor, D. Sweeney, L. Hale, W. Sweatt, and N. Wester, *Proceedings, 2nd International EUVL Workshop* (International Sematech, Austin, TX, 2000).
- ¹⁰P. Naulleau, K. Goldberg, E. Anderson, P. Batson, P. Denham, S. Rekawa, and J. Bokor, *Proc. SPIE* **4343**, 639 (2001).
- ¹¹P. Naulleau et al., *Proc. SPIE* **5374**, 881 (2004).
- ¹²P. Naulleau, P. Denham, B. Hoef, and S. Rekawa, *Opt. Commun.* **234**, 53 (2004).
- ¹³The flexure suspension galvanometers were manufactured by Nutfield Technology, Inc., 49 Range Road, Windham, NH 03087.
- ¹⁴S. Robertson et al., *Proc. SPIE* **5037**, 900 (2003).
- ¹⁵P. Naulleau, *Appl. Opt.* **43**, 788 (2004).
- ¹⁶S. Lee, D. Tichenor, P. Naulleau, and D. O'Connell, *J. Vac. Sci. Technol. B* **20**, 2849 (2002).